

# Inverse source in two-parameter anomalous diffusion, numerical algorithms and simulations over graded time-meshes

Khaled M. Furati<sup>a,b</sup>, Kassem Mustapha<sup>a,c</sup>, Ibrahim O. Sarumi<sup>a,d</sup>, Olaniyi S. Iyiola<sup>e</sup>

<sup>a</sup>*King Fahd University of Petroleum & Minerals  
Department of Mathematics & Statistics  
Dhahran 31261, Saudi Arabia*

<sup>b</sup>*kmfurati@kfupm.edu.sa*

<sup>c</sup>*kassem@kfupm.edu.sa*

<sup>d</sup>*isarumi@kfupm.edu.sa*

<sup>e</sup>*Department of Mathematics, Computer Science and Information Systems  
California University of Pennsylvania  
California, PA, USA  
iyiola@calu.edu*

## Abstract

We consider an inverse source two-parameter sub-diffusion model subject to a nonlocal initial condition. The problem models several physical processes, among them are the microwave heating and light propagation in photoelectric cells. A bi-orthogonal pair of bases is employed to construct a series representation of the solution and a Volterra integral equation for the source term. We develop a numerical algorithm for approximating the unknown time-dependent source term. Due to the singularity of the solution near  $t = 0$ , a graded mesh is used to improve the convergence rate. Numerical experiments are provided to illustrate the expected analytical order of convergence.

*Keywords:* Microwave heating; inverse source problem; anomalous diffusion; Volterra integral equation; collocation method; graded meshes.

## 1. Introduction

The main focus in this paper is to solve numerically the two-parameter time fractional diffusion inverse source problem:

$$\begin{aligned} D^{\alpha,\gamma}u(x,t) - u_{xx}(x,t) &= w(t)h(x,t), & 0 < x < 1, & \quad 0 < t \leq T, \\ I^{1-\gamma}u(x,t)|_{t=0} &= g(x), & 0 \leq x \leq 1, & \\ u(0,t) = u(1,t), & \quad u_x(1,t) = 0, & 0 < t \leq T, & \end{aligned} \quad (1)$$

with fractional exponents  $0 < \alpha \leq \gamma \leq 1$ . The functions  $h$  and  $g$  are given, while the solution  $u$  and the inverse source term  $w$  need to be determined. Thus, and for well-posedness, we have to impose an over-determination condition, defined by

$$\int_0^1 u(x,t)dx = q(t), \quad t \in [0, T]. \quad (2)$$

In the above model problem, the two-parameter fractional derivative operator  $D^{\alpha,\gamma}$  is defined by

$$D^{\alpha,\gamma}y(t) = D^\alpha \left( y(t) - \frac{I^{1-\gamma}y(0)}{\Gamma(\gamma)} t^{\gamma-1} \right),$$

where  $I^\mu$  and  $D^\mu$  are the Riemann-Liouville fractional integral and derivative, respectively. That is, for  $t > 0$  and  $0 < \mu < 1$ , with  $\omega_\mu(t) := t^{\mu-1}/\Gamma(\mu)$ ,

$$I^\mu y(t) = \int_0^t \omega_\mu(t-\tau)y(\tau) d\tau \quad \text{and} \quad D^\mu y(t) = \frac{d}{dt} I^{1-\mu} y(t).$$

When  $I^{1-\gamma}y$  is absolutely continuous, then  $D^{\alpha,\gamma}y = I^{\gamma-\alpha}D^\gamma y = I^{\gamma-\alpha}DI^{1-\gamma}y$ . Hence, when  $\gamma = \beta(1-\alpha) + \alpha$ ,  $0 < \beta \leq 1$ ,  $D^{\alpha,\gamma}$  reduces to the derivative introduced by Hilfer in [19]. Moreover,  $D^{\alpha,\alpha} = D^\alpha$  and  $D^{\alpha,1} = {}^cD^\alpha := I^{1-\alpha}D$ . Thus,  $D^{\alpha,\gamma}$  for  $\alpha \leq \gamma \leq 1$  is considered as an interpolant between the Riemann-Liouville fractional derivative  $D^\alpha$  and the Caputo fractional derivative  ${}^cD^\alpha$ .

Fractional PDEs open up new possibilities for robust mathematical modeling of physical processes that exhibit non-classical (non-Gaussian Lévy and non-Markovian processes; and non-Brownian transport phenomena) diffusion-dispersion. More precisely, fractional calculus provides a powerful tool for modeling a variety of nonlocal and memory-dependent phenomena. Such phenomena are recognized in many areas such as nanotechnology [4], control theory of dynamical systems [9, 30], viscoelasticity [27, 39], anomalous transport and diffusion [24], random walk dynamics [29], electrophysiology [11], image processing [25], and flow in porous media [3]. Some other physical and engineering processes are given in [33, 35] and more applications can be found in the surveys in [17, 23, 36]. In particular, fractional models are increasingly adopted for processes with anomalous diffusion [1, 28, 42]. The featured role of the fractional derivatives is mainly due to their non-locality nature which is an intrinsic property of many complex systems [18].

The problem (1) models several physical processes, among them is the microwave heating. When a material is irradiated with microwaves, the absorption of electromagnetic energy within the material increases its temperature. This effect can be modeled by replacing the electromagnetic power dissipation term in the nonlinear diffusion equation by an unknown equivalent internal heat source of the form  $w(t)h(x,t)$  [10]. The quantity  $q(t)$  in (2) represents the total absorbed energy due to the externally applied energy or it represents the total mass in the diffusion process of a chemical [7, 16, 20]. Knowing the local conversion rate of microwave energy  $h(x,t)$ , determining the source term  $w(t)$  gives an idea of how to control the external energy.

Inverse problems associated with models for anomalous diffusion processes arise in many applications. These problems include determining the initial conditions, boundary conditions, diffusion, fluxes and potential coefficients, fractional orders, and source terms. Such problems are in general ill-posed and some additional requirement or measurement are provided to make them well-posed. More details are given in [22].

When  $\gamma < 1$ , the non-local initial condition  $I^{1-\gamma}u(x,t)|_{t=0} = g(x)$  may lead to unbounded solution  $u$  of the model problem (1) near  $t = 0$ , this will definitely increase the level of complexity. However, when  $\gamma = 1$ , (one parameter Caputo derivative),  $I^{1-\gamma}u(x,t)|_{t=0}$  reduces to the standard (local) initial condition  $u(x,t)|_{t=0}$ . In this case, the inverse time-dependent source problems for fractional diffusion equation have been investigated under various initial, boundary and over determination conditions.

For unbounded spatial domains, Özkum *et al.* [34] used Adomian decomposition method to determine  $w(t)$  assuming that  $h(x,t) = 1$  (spatial variable diffusivity was allowed). Later, with  $h(x)$  in place of  $h(x,t)$ , Yang *et al.* [41] used the Fourier regularization method to obtain an a priori error estimate between the exact solution and its

regularized approximation.

For bounded domains and for  $h = h(x)$ , Sakamoto and Yamamoto [38] used eigenfunction expansions to prove a stability result for the inverse source problem of determining  $w(t)$ , with  $Lu$  in place of  $-u_{xx}$  where  $L$  is a linear symmetric elliptic operator. Wei and Zhang [40] solved numerically a Volterra integral equation (VIE) for  $w$  using boundary element method combined with a generalized Tikhonov regularization. For a different given data, Aleroev *et al.* [2], the Banach fixed-point theorem was used to prove the existence and uniqueness of  $w$ . For different given data and with  $h = h(x, t)$ , a similar framework was considered by Ismailov and Çiçek [21]. Furthermore, Demir *et al.* [12] recovered  $w$  by introducing input-output mappings and proved that their distinguishability holds under additional measurement data at a boundary point.

In all aforementioned cited works above, the problems considered involve the Caputo derivative together with the classical initial conditions. However, in problem (1), we consider a two parameter fractional derivative, of which, the Caputo and Riemann-Liouville derivatives are special cases, subject to nonlocal non-self adjoint boundary conditions and a nonlocal initial condition. Unlike the space-dependent source problems considered in [14, 15], this model gives rise to a VIE of the second kind for the source term  $w$ . This equation cannot be solved analytically due to the presence of a complicated weakly singular kernel as well as a right-hand side that involves a two parameter fractional derivative plus an infinite series, see (16). So, a numerical scheme based on the discontinuous collocation method is developed to approximate  $w$  by  $\tilde{w}$ .

Although we focused on finding a piecewise linear polynomial solution  $\tilde{w}$ , our approach can be extended to high-order polynomial solutions. For a smooth solution  $w$ , (that is, for smooth kernel  $E$ , smooth source  $G$ , and smooth coefficient  $H$  in (16)), the proposed scheme is second-order accurate globally. However, the solution  $w$  has singularity near  $t = 0$  due to the weak singularity in  $E$  and because the source term  $G$  is generally not bounded near  $t = 0$ . Thus, to achieve an optimal global  $O((\Delta t)^2)$  error ( $\Delta t$  is the maximum time step-size mesh element), we employ a non-uniform graded time meshes that based on concentrating the mesh elements near  $t = 0$  to compensate for the singular behavior of  $w$ , [6, 8, 31, 32]. The existence and uniqueness of the collocation solution  $\tilde{w}$  and the error bounds over graded time meshes are discussed. The numerical source  $\tilde{w}$  is used to approximate the solution  $u$  of (1).

The rest of the paper is organized as follows. In section 2, we introduce the bi-orthogonal basis and state some preliminary results. Section 3 focuses on deriving the integral equation for the source term  $w$  and on proposing a numerical algorithm for the numerical approximation of  $\tilde{w}$ . Existence, uniqueness and error analysis are investigated. Section 4 is devoted to seek an approximate solution of  $u$  using the approximate source term  $\tilde{w}$ . We ended the paper with some simulations in section 5.

## 2. Series Representations

As in [2], the non-self adjoint boundary conditions lead to the bi-orthogonal pair of bases  $\{\phi_{1,0}, \phi_{1,i}, \phi_{2,i}\}_{i=1}^{\infty}$  and  $\{\psi_{1,0}, \psi_{1,i}, \psi_{2,i}\}_{i=1}^{\infty}$  for the space  $L^2(0, 1)$ : with  $\lambda_i = 2\pi i$ ,

$$\phi_{10}(x) = 2, \quad \phi_{1i}(x) = 4(1 - x) \sin \lambda_i x, \quad \phi_{2i}(x) = 4 \cos \lambda_i x, \quad (3)$$

$$\psi_{10}(x) = x, \quad \psi_{1i}(x) = \sin \lambda_i x, \quad \psi_{2i}(x) = x \cos \lambda_i x. \quad (4)$$

We consider a series solution of the form

$$u(x, t) = u_{10}(t) \phi_{10}(x) + \sum_{\substack{i=1 \\ k=1,2}}^{\infty} u_{ki}(t) \phi_{ki}(x), \quad (5)$$

where

$$u_{10}(t) = \langle u, \psi_{10} \rangle, \quad u_{ki}(t) = \langle u, \psi_{ki} \rangle, \quad k = 1, 2, \quad i = 1, 2, \dots \quad (6)$$

Here,  $\langle \cdot, \cdot \rangle$  denotes the  $L^2(0, 1)$  inner product. Similarly, we let  $g_{ki}$  and  $h_{ki}(t)$  denote the series coefficients of  $g(x)$  and  $h(x, t)$  with respect to the basis functions in (3). Following [15], we assume that the functions  $g$  and  $h$  are sufficiently regular to guarantee the convergence of the series solution.

Substituting the series expansions of  $u$  and  $h$  in (1), we have

$$D^{\alpha, \gamma} u_{1i}(t) + \lambda_i^2 u_{1i}(t) = w(t) h_{1i}(t), \quad i \geq 0, \quad (7)$$

$$D^{\alpha, \gamma} u_{2i}(t) + \lambda_i^2 u_{2i}(t) + 2\lambda_i u_{1i}(t) = w(t) h_{2i}(t), \quad i \geq 1, \quad (8)$$

with  $\lambda_0 := 0$ . Moreover, from the initial condition in (1), we obtain the initial conditions

$$I^{1-\gamma} u_{10}(0) = g_{10}, \quad I^{1-\gamma} u_{ki}(0) = g_{ki}, \quad k = 1, 2, \quad i \geq 1. \quad (9)$$

Using Laplace transform and its inverse, the solution of these initial value problems are

$$u_{1i}(t) = (w h_{1i})(t) * \Theta_i^\alpha(t) + g_{1i} \Theta_i^\gamma(t), \quad i \geq 0, \quad (10)$$

and

$$\begin{aligned} u_{2i}(t) &= (w h_{2i})(t) * \Theta_i^\alpha(t) + g_{2i} \Theta_i^\gamma(t) \\ &\quad - 2\lambda_i \left[ (w h_{1i})(t) * (t^{2\alpha-1} E_{\alpha, 2\alpha}^2(-\lambda_i^2 t^\alpha)) + g_{1i} t^\sigma E_{\alpha, \alpha+\gamma}^2(-\lambda_i^2 t^\alpha) \right], \quad i \geq 1, \end{aligned} \quad (11)$$

where the convolution

$$f(t) * g(t) := \int_0^t f(\tau) g(t - \tau) d\tau \quad \text{and} \quad \Theta_i^\gamma(t) := t^{\gamma-1} E_{\alpha, \gamma}(-\lambda_i^2 t^\alpha).$$

Here, the generalized Mittag-Leffler function [37] is defined by

$$E_{\alpha, \beta}^\rho(t) = \sum_{k=0}^{\infty} \frac{\Gamma(\rho + k)}{\Gamma(\rho) \Gamma(\alpha k + \beta)} \frac{t^k}{k!}. \quad (12)$$

Therefore, once the source term  $w(t)$  is determined, the series coefficients of the solution  $u(x, t)$  can be computed. In the next section, we discuss the determination and approximation of  $w(t)$ .

### 3. Determination and approximation of $w$ .

This section is devoted to discuss the process of approximating the source term  $w(t)$  in (1). It turns out that  $w$  satisfies a VIE of the second kind with variable coefficients. Due to the complexity in solving this integral equation analytically, the numerical solution of  $w$  via a discontinuous collocation method is investigated.

### 3.1. Integral equation

Integrating the first equation in (1) over the spatial domain  $[0, 1]$  and using the given boundary conditions, we obtain for  $0 < t < T$  that

$$H(t)w(t) = \int_0^1 D^{\alpha,\gamma}u(x,t)dx + u_x(0,t), \quad \text{where } H(t) = \int_0^1 h(x,t)dx. \quad (13)$$

From condition (2),

$$\int_0^1 D^{\alpha,\gamma}u(x,t)dx = D^{\alpha,\gamma} \int_0^1 u(x,t)dx = D^{\alpha,\gamma}q(t), \quad (14)$$

and thus,

$$H(t)w(t) = D^{\alpha,\gamma}q(t) + u_x(0,t), \quad 0 < t < T. \quad (15)$$

For the second term on the right hand side of (13), the series representation of  $u(x,t)$  in (5) and the associated coefficients (10) yield

$$\begin{aligned} u_x(0,t) &= 4 \sum_{n=1}^{\infty} \lambda_i u_{1i}(t) = 4 \sum_{i=1}^{\infty} \lambda_i \left\{ g_{1i} \Theta_i^\gamma(t) + (w h_{1i})(t) * \Theta_i^\alpha(t) \right\} \\ &= 4 \sum_{i=1}^{\infty} \lambda_i g_{1i} \Theta_i^\gamma(t) + \int_0^t w(\tau) \sum_{i=1}^{\infty} 4 \lambda_i h_{1i}(\tau) \Theta_i^\alpha(t-\tau) d\tau. \end{aligned}$$

Inserting this in (15) amounts to the following VIE of the second kind:

$$H(t)w(t) - \int_0^t E(t,\tau)w(\tau)d\tau = G(t), \quad (16)$$

where

$$E(t,\tau) = 4 \sum_{i=1}^{\infty} \lambda_i h_{1i}(\tau) \Theta_i^\alpha(t-\tau), \quad (17)$$

and

$$G(t) = D^{\alpha,\gamma}q(t) + 4 \sum_{i=1}^{\infty} \lambda_i g_{1i} \Theta_i^\gamma(t). \quad (18)$$

Note that the kernel  $E$  can be written in the form

$$E(t,\tau) = (t-\tau)^{\alpha-1} \tilde{E}(t,\tau), \quad \tilde{E}(t,\tau) = 4 \sum_{i=1}^{\infty} \lambda_i h_{1i}(\tau) E_{\alpha,\alpha}(-\lambda_i^2(t-\tau)^\alpha). \quad (19)$$

Since  $|E_{\alpha,\alpha}(-\lambda_i^2 s^\alpha)| \leq \frac{C}{1 + \lambda_i^2 s^\alpha}$ ,

$$|\tilde{E}(t,\tau)| \leq C \sum_{i=1}^{\infty} \lambda_i^{-1} h_{1i}(\tau) \leq C, \quad (20)$$

where the second inequality is valid provided that  $h(x,t)$  has a finite number of Fourier-modes or is sufficiently regular (for instance,  $h_{1i}(\tau) \leq C\lambda_i^{-2-\epsilon}$  for some positive  $\epsilon$ ), see [15] for more details. As a consequence,  $\tilde{E}(\cdot, \cdot)$  is continuous on  $[0, T] \times [0, T]$ . Also, for

sufficiently regular functions  $g$  and  $q$ , one can check that the function  $G$  is continuous on  $[\epsilon, T]$  for  $0 < \epsilon < T$ . This guarantees the existence and uniqueness of the continuous solution  $w_\epsilon$  of (16) on the interval  $[\epsilon, T]$ , for more details, we refer the reader to [5, Chapter 6] or [26, Section 3.4]. In the limiting case,  $\epsilon$  approaches 0, the existence and uniqueness of the continuous solution  $w$  of (16) on  $(0, T]$  follows.

The numerical solution of (16) via a discontinuous collocation method will be investigated in the next subsection. The upper bound in (20) is used below to derive the error estimates for our discretization.

### 3.2. Approximation of $w(t)$

We intend to approximate the solution  $w$  of (16) by piecewise linear polynomials via a robust discontinuous collocation method. To do so, we introduce a time partition of the interval  $[0, T]$  given by the graded nodes  $t_n = (n/N)^\delta T$  (with  $\delta \geq 1$ ) for  $0 \leq n \leq N$ . Let  $I_n = (t_{n-1}, t_n]$  and  $\Delta t_n = t_n - t_{n-1}$ ,  $1 \leq n \leq N$ , with  $\Delta t := \max_{1 \leq n \leq N} \Delta t_n$ .

Let  $S$  be the finite dimensional space of linear polynomials on each time mesh element  $I_n$ ,  $1 \leq n \leq N$ . The set of collocation (grid) points is

$$X = \left\{ t_{n,j} := t_{n-1} + \xi_j \Delta t_n, \quad 1 \leq j \leq 2, \quad n = 1, \dots, N \right\}, \quad 0 < \xi_1 < \xi_2 < 1.$$

One option is to choose  $\xi_1$  and  $\xi_2$  to be the Gauss quadrature points.

The discontinuous collocation solution  $\tilde{w} \in S$  is now defined by

$$H(t) \tilde{w}(t) - \int_0^t E(t, \tau) \tilde{w}(\tau) d\tau = G(t), \quad t \in X. \quad (21)$$

Alternatively, this scheme can be rewritten as: for  $j = 1, 2$ , and  $n = 1, \dots, N$ ,

$$H(t_{n,j}) \tilde{w}(t_{n,j}) - \int_0^{t_{n,j}} E(t_{n,j}, \tau) \tilde{w}(\tau) d\tau = G(t_{n,j}). \quad (22)$$

On each subinterval  $I_n$ , we will base the computational form of  $\tilde{w}$  on the Lagrange basis functions with respect to the collocation parameters  $\{\xi_1, \xi_2\}$ . That is,

$$\tilde{w}(t) = \tilde{w}(t_{n,1}) L_{n,1}(t) + \tilde{w}(t_{n,2}) L_{n,2}(t), \quad t \in I_n, \quad (23)$$

where for each fixed  $n$ ,  $\{L_{n,j}\}_{j=1,2}$  are the local Lagrange basis functions associated with the collocation points  $\{t_{n,j}\}_{j=1,2}$  corresponding to the interval  $I_n$  defined by

$$L_{n,1}(t) = \frac{t_{n,2} - t}{\zeta_n} \quad \text{and} \quad L_{n,2}(t) = \frac{t - t_{n,1}}{\zeta_n}, \quad \zeta_n = t_{n,2} - t_{n,1}. \quad (24)$$

To handle the integral term in (22), we use the definition  $\tilde{w}$  given in (23) and obtain,

$$\begin{aligned} \int_0^{t_{n,j}} E(t_{n,j}, \tau) \tilde{w}(\tau) d\tau &= \sum_{s=1}^2 \sum_{m=1}^n \tilde{w}(t_{m,s}) \int_{t_{m-1}}^{\min\{t_{n,j}, t_m\}} E(t_{n,j}, \tau) L_{m,s}(\tau) d\tau \\ &= \sum_{s=1}^2 \sum_{m=1}^n a_{m,s}(t_{n,j}) \tilde{w}(t_{m,s}), \end{aligned}$$

where, for  $1 \leq m \leq n$ ,

$$a_{m,s}(t_{n,j}) = \int_{t_{m-1}}^{\min\{t_{n,j}, t_m\}} E(t_{n,j}, \tau) L_{m,s}(\tau) d\tau.$$

Thus the numerical scheme in (22) can be written as

$$H(t_{n,j}) \tilde{w}(t_{n,j}) - \sum_{s=1}^2 a_{n,s}(t_{n,j}) \tilde{w}^{n,s} = F^{n,j}, \quad j = 1, 2, \quad n = 1, \dots, N, \quad (25)$$

with

$$F^{n,j} = G(t_{n,j}) + \sum_{s=1}^2 \sum_{m=1}^{n-1} a_{m,s}(t_{n,j}) \tilde{w}(t_{m,s}).$$

Therefore, for each  $n$ , we have to solve the  $2 \times 2$  linear system

$$(\mathbf{H}^n - \mathbf{B}^n) \begin{bmatrix} \tilde{w}(t_{n,1}) \\ \tilde{w}(t_{n,2}) \end{bmatrix} = \mathbf{F}^n := \begin{bmatrix} F^{n,1} \\ F^{n,2} \end{bmatrix}, \quad (26)$$

with

$$\mathbf{H}^n = \begin{bmatrix} H(t_{n,1}) & 0 \\ 0 & H(t_{n,2}) \end{bmatrix}, \quad \mathbf{B}^n = \begin{bmatrix} a_{n,1}(t_{n,1}) & a_{n,2}(t_{n,1}) \\ a_{n,1}(t_{n,2}) & a_{n,2}(t_{n,2}) \end{bmatrix}.$$

Since our discontinuous collocation scheme (21) amounts to a 2-by-2 linear system on each time mesh element  $I_n$ , the existence of the solution  $\tilde{w}$  follows from its uniqueness. To guarantee the uniqueness of  $\tilde{w}$ , it is clear from (26) that we need the matrix  $\mathbf{H}^n - \mathbf{B}^n$  to be non-singular. However, the kernel is weakly singular of order  $\alpha - 1$ , then for any  $0 < \alpha \leq 1$ , there exists  $k_\alpha > 0$  such that the non-singularity of the matrix  $\mathbf{H}^n - \mathbf{B}^n$  can be assured whenever  $\Delta t < k_\alpha$ , provided the matrix  $H$  is non-singular.

The collocation scheme (22) is yet fully discrete due to the integrals in the entries of the matrix  $\mathbf{B}^n$  and the vector  $\mathbf{F}^n$ . To compute these entries, we approximate the Fourier coefficient  $h_{1i}(t)$ ,  $i = 1, 2, \dots$  by its midpoint average value on each time subinterval  $I_n$  and the remaining part of the integral can be computed exactly. This approximation preserves the second order of accuracy (over nonuniform meshes) of the collocation scheme in the presence of the weakly singular kernel  $E$ . Explicitly, for  $1 \leq n, m \leq N$ , and for  $j, s \in \{1, 2\}$ ,

$$\begin{aligned} a_{m,s}(t_{n,j}) &= 4 \int_{t_{m-1}}^{\min\{t_{n,j}, t_m\}} \sum_{i=1}^{\infty} \lambda_i h_{1i}(\tau) \Theta_i^\alpha(t_{n,j} - \tau) L_{m,s}(\tau) d\tau \\ &\approx 4 \sum_{i=1}^{\infty} \lambda_i h_{1i}^{m-1/2} \int_{t_{m-1}}^{\min\{t_{n,j}, t_m\}} \Theta_i^\alpha(t_{n,j} - \tau) L_{m,s}(\tau) d\tau \\ &= 4 \sum_{i=1}^{\infty} \lambda_i h_{1i}^{m-1/2} \int_{t_{m-1}}^{\min\{t_{n,j}, t_m\}} (t_{n,j} - \tau)^{\alpha-1} E_{\alpha,\alpha}(-\lambda_i^2(t_{n,j} - \tau)) L_{m,s}(\tau) d\tau \\ &= 4 \sum_{i=1}^{\infty} \frac{1}{\lambda_i} h_{1i}^{m-1/2} \Psi^\alpha(t_{n,j}, \tau, \lambda_i^2, L_{m,s}) \Big|_{t_{m-1}}^{\min\{t_{n,j}, t_m\}}, \end{aligned}$$

where the integral formula in the lemma below is used in the last equality.

**Lemma 3.1.** For any linear polynomial  $L(t) = \nu t + c$ , we have

$$\lambda \int_a^b (t - \tau)^{\alpha-1} E_{\alpha,\alpha}(-\lambda(t - \tau)^\alpha) L(\tau) d\tau = \Psi^\alpha(t, \tau, \lambda, L) \Big|_{\tau=a}^{\tau=b}, \quad (27)$$

where

$$\Psi^\alpha(t, \tau, \lambda, L) = E_\alpha(-\lambda(t - \tau)^\alpha) L(\tau) + \nu (t - \tau) E_{\alpha,2}(-\lambda(t - \tau)^\alpha).$$

*Proof.* Recall the following formulas: if  $\alpha, \beta, \lambda \in \mathbb{C}$  such that  $\text{Re}(\alpha) > 0$  then

$$\begin{aligned} \lambda t^\alpha E_{\alpha,\alpha+\beta}(-\lambda t^\alpha) &= \frac{1}{\Gamma(\beta)} - E_{\alpha,\beta}(-\lambda t^\alpha), \\ \int (t - \tau)^{\beta-1} E_{\alpha,\beta}^\rho(-\lambda(t - \tau)^\alpha) d\tau &= -(t - \tau)^\beta E_{\alpha,\beta+1}^\rho(-\lambda(t - \tau)^\alpha) + C. \end{aligned}$$

Integrating by parts, and then using the second formula followed by the first one, we notice that

$$\begin{aligned} &\lambda \int (t - \tau)^{\alpha-1} E_{\alpha,\alpha}(-\lambda(t - \tau)^\alpha) L(\tau) d\tau \\ &= -\lambda(t - \tau)^\alpha E_{\alpha,\alpha+1}(-\lambda(t - \tau)^\alpha) L(\tau) + \lambda \nu \int (t - \tau)^\alpha E_{\alpha,\alpha+1}(-\lambda(t - \tau)^\alpha) d\tau \\ &= -\lambda(t - \tau)^\alpha E_{\alpha,\alpha+1}(-\lambda(t - \tau)^\alpha) L(\tau) - \lambda \nu (t - \tau)^{\alpha+1} E_{\alpha,\alpha+2}(-\lambda(t - \tau)^\alpha) \\ &= [E_\alpha(-\lambda(t - \tau)^\alpha) - 1] L(\tau) + \nu (t - \tau) [E_{\alpha,2}(-\lambda(t - \tau)^\alpha) - 1]. \end{aligned}$$

Since  $L(\tau) + \nu(t - \tau) \Big|_{\tau=a}^{\tau=b} = 0$ , the desired result follows.  $\square$

### 3.3. Error analysis

As mentioned earlier, for VIEs with a smooth kernel and source term, the collocation scheme is  $O((\Delta t)^2)$  accurate. However, due to the lack of regularity of the continuous solution  $w$  (has singularity near  $t = 0$ ) caused by the presence of the weakly singular kernel  $E$  and the nonsmooth source term  $G$ , such order of accuracy is not feasible over uniform meshes. For this reason and to improve the convergence rates, a graded mesh with time nodes  $t_n = (n/N)^\delta T$  ( $\delta \geq 1$ ) is employed [31, 32] to compensate for the singular behavior of  $w$  near  $t = 0$ .

Next, a concise proof of the error estimates from the discontinuous collocation discretization over the graded mesh  $t_n = (n/N)^\delta T$  (with  $\delta \geq 1$ ) is given. We impose the following typical assumption on the derivative of the continuous solution  $w$ ; for some  $0 < \sigma < 1$  and for  $t > 0$ ,

$$|w(t)| \leq a(1 + t^\alpha) + bt^{\gamma-1} \quad \text{and} \quad |w'(t)| + t|w''(t)| \leq C t^{\sigma-1}, \quad (28)$$

for some constants  $a, b$ .

**Remark.** Under reasonable assumptions on the given data, the above regularity conditions can be verified, where typically  $\sigma = \alpha + \gamma - 1$  and so, we require  $\alpha + \gamma > 1$ . Another note, in the presence of the two-parameter fractional derivative  $D^{\alpha,\gamma}$  ( $\gamma < 1$ ), the solution  $w$  has a strong singularity near  $t = 0$ . More precisely,  $w$  is not bounded



near  $t = 0$  and  $w'$  is not integrable on  $[0, T]$  (unless  $\sigma > 0$ ). Therefore, efficient approximations of  $w$  on the first sub-interval  $I_1$  require more effort. One way, is to inherit the order of singularity (that is due to  $\gamma$ ) in the approximate solution, for instance, approximate  $w$  by the function  $a_1 + a_2 t^{\gamma-1}$  on  $I_1$ . Investigating this is beyond the scope of this paper and it will be a topic of future research. On the other hand, it is worth to mention that for the case of Caputo derivative,  $\gamma = 1$ ,  $w$  is uniformly bounded on  $[0, T]$  and  $w'$  is integrable on  $[0, T]$ .

Decomposing the error  $w - \tilde{w}$  as

$$w - \tilde{w} = (w - Pw) + (Pw - \tilde{w}) =: \eta_1 + \eta_2,$$

where the comparison function  $Pw \in S$  interpolates  $w$  at the composite Gauss-quadrature nodes, that is,

$$Pw(t) = w(t_{n,1})L_{n,1}(t) + w(t_{n,2})L_{n,2}(t), \quad t \in I_n, \quad 1 \leq n \leq N. \quad (29)$$

It is known that

$$\|\eta_1\|_{L^\infty(I_n)} \leq C(\Delta t_n)^{j-1} \int_{I_n} |w^{(j)}(t)| dt, \quad j = 1, 2.$$

Hence, by the regularity assumption (28) on  $w$  we have

$$\|\eta_1\|_{L^\infty(I_1)} \leq C \int_{I_1} t^{\sigma-1} dt < Ck_1^\sigma \leq C(\Delta t)^{\sigma\delta}.$$

Furthermore, for  $n \geq 2$ , using the mesh properties;  $t_n \leq Ct_{n-1}$  and  $\Delta t_n \leq k t_n^{1-1/\delta}$ , we notice that

$$\|\eta_1\|_{L^\infty(I_n)} \leq C(\Delta t_n)^2 t_n^{\alpha+\gamma-3} = C(\Delta t_n/t_n)^{\sigma\delta} (\Delta t_n/t_n)^{2-\sigma\delta} t_n^\sigma \leq C(\Delta t)^{\sigma\delta},$$

for  $0 < \sigma\delta \leq 2$ . Therefore, for  $1 \leq n \leq N$ ,

$$\|\eta_1\|_{L^\infty(I_n)} \leq C(\Delta t)^{\sigma\delta}, \quad \text{for } 1 \leq \delta \leq 2/\sigma.$$

To estimate the second term  $\eta_2$ , we notice from (16), (21) and the definition of  $Pw$  that

$$H(t)\eta_2(t) - \int_0^t E(t, \tau) \eta_2(\tau) d\tau = \int_0^t E(t, \tau) \eta_1(\tau) d\tau, \quad t \in X. \quad (30)$$

Using  $|E(t, \tau)| \leq C(t - \tau)^{\alpha-1}$  for  $t < \tau$  (see (19)–(20)), after some manipulations and for a sufficiently small step size  $k$ , the above equation amounts to

$$|\eta_2(t_{n,j})| \leq C \max_{1 \leq j \leq n} \|\eta_1\|_{L^\infty(I_j)} \int_0^{t_{n,j}} E(t_{n,j}, \tau) d\tau + C \sum_{i=1}^{n-1} \int_{t_{i-1}}^{t_i} (t_{n,j} - \tau)^{\alpha-1} d\tau \sum_{\ell=1}^2 |\eta_2(t_{i,\ell})|,$$

for  $1 \leq n \leq N$  and for  $j = 1, 2$ . Thus, an application of the weakly singular discrete Gronwall inequality [13, Theorem 6.1] gives

$$|\eta_2(t_{n,j})| \leq C \max_{1 \leq j \leq n} \|\eta_1\|_{L^\infty(I_j)} \int_0^{t_{n,j}} E(t_{n,j}, \tau) d\tau \leq C \max_{1 \leq j \leq n} \|\eta_1\|_{L^\infty(I_j)}.$$

Next, the expansion of  $\tilde{w}$  given in (23) and the achieved estimate of  $\eta_1$  yield

$$\|\eta_2\|_{L^\infty(I_n)} \leq C(\Delta t)^{\sigma\delta}, \quad \text{for } 1 \leq \delta \leq 2/\sigma, \quad \text{for } 1 \leq n \leq N,$$

and consequently, we attain the following error bound, for  $\alpha + \gamma > 1$ ,

$$\|w - \tilde{w}\|_{L^\infty(I_n)} \leq C(\Delta t)^{\sigma\delta}, \quad \text{for } 1 \leq \delta \leq 2/\sigma, \quad \text{for } 1 \leq n \leq N.$$

The above error bound shows that a global optimal  $O((\Delta t)^2)$  convergence rates can be recovered by choosing the graded mesh exponent  $\delta$  to be  $2/\sigma$ .

#### 4. Approximation of $u$

This section is devoted to discuss the numerical approximation of the solution  $u$  of the fractional model problem (1), denoted by  $\tilde{u}$ . More precisely, we approximate the Fourier coefficients  $u_{ki}$  for  $k = 1, 2$  in equations (10) and (11) by  $\tilde{u}_{ki}$  using the (source term) collocation solution  $\tilde{w}$ . Thus,

$$\begin{aligned} \tilde{u}_{1i}(t) &\approx (\tilde{w} h_{1i})(t) * \Theta_i^\alpha(t) + g_{1i} \Theta_i^\gamma(t), \quad i \geq 0, \\ \tilde{u}_{2i}(t) &\approx (\tilde{w} h_{2i})(t) * \Theta_i^\alpha(t) + g_{2i} \Theta_i^\gamma(t) \\ &\quad - 2\lambda_i [(\tilde{w} h_{1i})(t) * (t^{2\alpha-1} E_{\alpha,2\alpha}^2(-\lambda_i^2 t^\alpha)) + g_{1i} t^\sigma E_{\alpha,\alpha+\gamma}^2(-\lambda_i^2 t^\alpha)], \quad i \geq 1. \end{aligned}$$

Following the convention in the previous subsection, we approximate the convolutions as follows:

$$\begin{aligned} (\tilde{w} h_{1i})(t_n) * \Theta_i^\alpha(t_n) &\approx \sum_{m=1}^n h_{1i}^{m-1/2} \int_{t_{m-1}}^{t_m} \Theta_i^\alpha(t_n - \tau) \sum_{s=1}^2 \tilde{w}(t_{m,s}) L_{m,s}(\tau) d\tau \\ &= \sum_{m=1}^n h_{1i}^{m-1/2} \sum_{s=1}^2 \tilde{w}(t_{m,s}) \int_{t_{m-1}}^{t_m} \Theta_i^\alpha(t_n - \tau) L_{m,s}(\tau) d\tau. \end{aligned}$$

Hence, for  $i > 0$

$$\tilde{u}_{1i}(t_n) \approx \sum_{m=1}^n \frac{h_{1i}^{m-1/2}}{\lambda_i^2} \sum_{s=1}^2 \tilde{w}(t_{m,s}) \Psi^\alpha(t_n, \tau, \lambda_i^2, L_{m,s}) \Big|_{t_{m-1}}^{t_m} + g_{1i} \Theta_i^\gamma(t_n).$$

In a similar fashion, the first two terms in  $\tilde{u}_{2i}$  can be computed (just replace  $h_{1i}$  and  $g_{1i}$  with  $h_{2i}$  and  $g_{2i}$ , respectively, in the above equation).

It remains to compute  $\tilde{u}_{10}$  and the second convolution term in  $\tilde{u}_{2i}$ . For  $i = 0$ ,

$$\begin{aligned} (\tilde{w} h_{10} * \omega_\alpha)(t_n) &\approx \sum_{m=1}^n h_{10}^{m-1/2} \int_{t_{m-1}}^{t_m} \tilde{w}(\tau) \omega_\alpha(t_n - \tau) d\tau \\ &\approx \sum_{m=1}^n h_{10}^{m-1/2} \sum_{s=1}^2 \tilde{w}(t_{m,s}) \int_{t_{m-1}}^{t_m} L_{m,s}(\tau) \omega_\alpha(t_n - \tau) d\tau, \end{aligned}$$

and thus,

$$\begin{aligned} \tilde{u}_{10}(t_n) &= (w h_{10} * \omega_\alpha)(t_n) + g_{10} \omega_\gamma(t_n) \approx \sum_{m=1}^n h_{10}^{m-1/2} \sum_{s=1}^2 \tilde{w}(t_{m,s}) \times \\ &\quad \left( L_{m,s}(\tau) \omega_{\alpha+1}(t_n - \tau) + \frac{(-1)^s}{\zeta_m} \omega_{\alpha+2}(t_n - \tau) \right) \Big|_{t_m}^{t_{m-1}} + g_{10} \omega_\gamma(t_n). \end{aligned}$$

Similarly, we compute the second convolution term in  $\tilde{u}_{2i}$ , and get

$$[(\tilde{w} h_{1i})(t_n) * (t_n^{2\alpha-1} E_{\alpha,2\alpha}^2(-\lambda_i^2 t_n^\alpha))] \approx \sum_{m=1}^n h_{1i}^{m-1/2} \sum_{s=1}^2 \tilde{w}(t_{m,s}) \mathcal{T}_{\alpha,n}^m$$

with

$$\begin{aligned} \mathcal{T}_{m,s}^{\alpha,n} &:= \int_{t_{m-1}}^{t_m} L_{m,s}(\tau) (t_n - \tau)^{2\alpha-1} E_{\alpha,2\alpha}^2(-\lambda_i^2 (t_n - \tau)^\alpha) d\tau \\ &= -L_{m,s}(\tau) (t_n - \tau)^{2\alpha} E_{\alpha,2\alpha+1}^2(-\lambda_i^2 (t_n - \tau)^\alpha) \Big|_{t_{m-1}}^{t_m} \\ &\quad - \frac{(-1)^s}{\zeta_m} (t_n - \tau)^{2\alpha+1} E_{\alpha,2\alpha+2}^2(-\lambda_i^2 (t_n - \tau)^\alpha) \Big|_{t_{m-1}}^{t_m}. \end{aligned}$$

In the second equality, we integrated by parts and used the second formula in the proof of Lemma 3.1. By Combining the above contributions, we complete the computation of  $\tilde{u}_{2i}$ .

## 5. Numerical results

This section is devoted to illustrate numerically the convergence of the proposed discontinuous collocation scheme for the VIE of the form (16) and to compare between the analytical solution  $u$  of (1) and its approximation  $\tilde{u}$ . For this purpose and to be able to compute  $w$  and  $u$  exactly, we consider problem (1) with  $T = 1$  and

$$\begin{aligned} g(x) &= 4 \cos(4\pi x), \\ q(t) &= \omega_{1+\alpha}(t), \\ h(x, t) &= \frac{\lambda_1^2 - 1}{\lambda_1^2} + \frac{(1-x) \sin(2\pi x)}{\lambda_1} + 4t \cos(2\pi x) + 8 \cos(4\pi x). \end{aligned}$$

The only nonzero series coefficients of  $h(x, t)$  and  $g(x)$  are

$$h_{10} = \frac{\lambda_1^2 - 1}{2\lambda_1^2}, \quad h_{11} = \frac{1}{4\lambda_1}, \quad h_{21}(t) = t, \quad h_{22}(t) = 2, \quad g_{22} = 1. \quad (31)$$

Furthermore, for this choice of  $h(x, t)$  and  $q(t)$ , we have

$$H(t) = \int_0^1 h(x, t) dx = 2 \frac{\lambda_1^2 - 1}{2\lambda_1^2} + \frac{1}{\lambda_1^2} = 1 \quad \text{and} \quad D^{\alpha,\gamma} q(t) = D^\alpha q(t) = 1. \quad (32)$$

Inserting these terms in (17) and (18), we reach

$$E(t, \tau) = \Theta_1^\alpha(t - \tau) \quad \text{and} \quad G(t) = D^{\alpha,\gamma} q(t) + \sum_{i=1}^{\infty} 4\lambda_i g_{1i} \Theta_i^\gamma(t) = 1.$$

Therefore, the VIE (16) reduces to  $w(t) - (w * \Theta_1^\alpha)(t) = 1$ . To find  $w$ , we take Laplace transform of both sides and use the formula

$$\mathcal{L}\{t^{\beta-1} E_{\alpha,\beta}(at^\alpha)\}(s) = \frac{s^{\alpha-\beta}}{s^\alpha - a}, \quad \alpha, \beta > 0. \quad (33)$$

Let  $W$  denotes Laplace transform of  $w$ , then

$$W(s) = \frac{1}{s} \frac{s^\alpha + \lambda_1^2}{s^\alpha + \lambda_1^2 - 1} = \frac{1}{\lambda_1^2 - 1} \left[ \frac{\lambda_1^2}{s} - \frac{s^{\alpha-1}}{s^\alpha + \lambda_1^2 - 1} \right]. \quad (34)$$

By taking the inverse Laplace transform, the exact source term is given by

$$w(t) = \frac{1}{\lambda_1^2 - 1} [\lambda_1^2 - E_\alpha((1 - \lambda_1^2)t^\alpha)]. \quad (35)$$

Next, we find the series coefficients for the solution  $u(x, t)$ . By (10), (11) and (31),

$$u_{1i}(t) = h_{1i}(w * \Theta_i^\alpha)(t) \text{ for } i = 0, 1, \text{ and } u_{1i} = 0 \text{ for } i \geq 2, \quad (36)$$

and

$$u_{2i}(t) = \begin{cases} (tw(t)) * \Theta_1^\alpha(t) - \frac{1}{2}w(t) * (t^{2\alpha-1}E_{\alpha,2\alpha}(-\lambda_1^2t^\alpha)), & i = 1, \\ 2(w * \Theta_2^\alpha)(t) + \Theta_2^\gamma(t), & i = 2, \\ 0, & i \geq 3. \end{cases} \quad (37)$$

Therefore, the exact solution is given by

$$u(x, t) = 2u_{10}(t) + 4(1 - x) \sin(\lambda_1 x) u_{11}(t) + 4 \cos(\lambda_1 x) u_{21}(t) + 4 \cos(\lambda_2 x) u_{22}(t). \quad (38)$$

We compute the convolutions in (36) and (37) through the Laplace transform. For  $i \geq 0$ , using the formula in (33) and the achieved contribution in (34) yield

$$\begin{aligned} (\mathcal{L}(w * \Theta_i^\alpha))(s) &= W(s) (\mathcal{L}\Theta_i^\alpha)(s) = \frac{s^{\alpha-1} + \lambda_1^2 s^{-1}}{s^\alpha + \lambda_1^2 - 1} \frac{1}{s^\alpha + \lambda_i^2} \\ &= \frac{1}{\lambda_i^2 - \lambda_1^2 + 1} \left[ \frac{s^{\alpha-1}}{s^\alpha + \lambda_1^2 - 1} + \frac{\lambda_1^2 s^{-1}}{s^\alpha + \lambda_1^2 - 1} - \frac{s^{\alpha-1}}{s^\alpha + \lambda_i^2} - \frac{\lambda_1^2 s^{-1}}{s^\alpha + \lambda_i^2} \right]. \end{aligned}$$

By taking inverse Laplace transform, we have, for  $i \geq 0$ ,

$$\begin{aligned} (w * \Theta_i^\alpha)(t) &= \frac{1}{\lambda_i^2 - \lambda_1^2 + 1} \times \\ &[E_\alpha((1 - \lambda_1^2)t^\alpha) + \lambda_1^2 t^\alpha E_{\alpha,\alpha+1}((1 - \lambda_1^2)t^\alpha) - E_\alpha(-\lambda_i^2)t^\alpha - \lambda_1^2 t^\alpha E_{\alpha,\alpha+1}((-\lambda_i^2)t^\alpha)]. \end{aligned}$$

Noting that, for  $i \geq 1$ , using the shifting identity of the Mittag-Leffler function,

$$(w * \Theta_i^\alpha)(t) = \frac{1}{\lambda_i^2 - \lambda_1^2 + 1} \left[ \frac{E_\alpha((1 - \lambda_1^2)t^\alpha)}{1 - \lambda_1^2} + \frac{\lambda_1^2 - \lambda_i^2}{\lambda_i^2} E_\alpha(-\lambda_i^2)t^\alpha + k_2 - \frac{\lambda_1^2}{\lambda_i^2} \right].$$

It remains to compute the convolution terms in  $u_{21}$ . For convenience, putting  $k_1 = 1/(\lambda_1^2 - 1)$  and  $k_2 = \lambda_1^2 k_1$ . Using  $\mathcal{L}\{tw(t)\}(s) = -W'(s)$ , then from (34), we have

$$\mathcal{L}\{tw(t)\}(s) = \frac{k_2}{s^2} + \frac{(\alpha - 1) s^{\alpha-2}}{(s^\alpha + (\lambda_1^2 - 1))^2} - \frac{k_1 s^{2\alpha-2}}{(s^\alpha + (\lambda_1^2 - 1))^2}.$$

Accordingly,

$$\begin{aligned} \mathcal{L}\{(tw(t)) * \Theta_1^\alpha(t)\}(s) &= \left[ \frac{k_2}{s^2} + \frac{(\alpha - 1) s^{\alpha-2}}{(s^\alpha + (\lambda_1^2 - 1))^2} - \frac{k_1 s^{2\alpha-2}}{(s^\alpha + (\lambda_1^2 - 1))^2} \right] \frac{1}{s^\alpha + \lambda_1^2} \\ &= \frac{k_2 s^{-2}}{s^\alpha + \lambda_1^2} + [(\alpha - 1)s^{\alpha-2} - k_1 s^{2\alpha-2}] \left[ \frac{1}{s^\alpha + \lambda_1^2} - \frac{1}{s^\alpha + (\lambda_1^2 - 1)} + \frac{1}{(s^\alpha + (\lambda_1^2 - 1))^2} \right]. \end{aligned}$$

Thus,

$$\begin{aligned} (tw(t)) * \Theta_1^\alpha(t) &= k_2 t^{1+\alpha} E_{\alpha,2+\alpha}(-\lambda_1^2 t^\alpha) \\ &\quad + (\alpha - 1) [t E_{\alpha,2}(-\lambda_1^2 t^\alpha) - t E_{\alpha,2}((1 - \lambda_1^2)t^\alpha) + t^{\alpha+1} E_{\alpha,2+\alpha}^2((1 - \lambda_1^2)t^\alpha)] \\ &\quad - k_1 [t^{1-\alpha} E_{\alpha,2-\alpha}(-\lambda_1^2 t^\alpha) - t^{1-\alpha} E_{\alpha,2-\alpha}((1 - \lambda_1^2)t^\alpha) + t E_{\alpha,2}^2((1 - \lambda_1^2)t^\alpha)]. \end{aligned}$$

For the second convolution term in  $u_{21}$ , since

$$\begin{aligned} \mathcal{L}\left\{w(t) * (t^{2\alpha-1} E_{\alpha,2\alpha}^2(-\lambda_1^2 t^\alpha))\right\}(s) &= k_1 \left[ \frac{\lambda_1^2}{s} - \frac{s^{\alpha-1}}{s^\alpha + \lambda_1^2 - 1} \right] \frac{1}{(s^\alpha + \lambda_1^2)^2} \\ &= k_1 \left[ \frac{\lambda_1^2}{s(s^\alpha + \lambda_1^2)^2} + \frac{s^{\alpha-1}}{(s^\alpha + \lambda_1^2)^2} + \frac{s^{\alpha-1}}{(s^\alpha + \lambda_1^2)^2} - \frac{s^{\alpha-1}}{s^\alpha + (\lambda_1^2 - 1)} \right], \end{aligned}$$

$$\begin{aligned} w(t) * (t^{2\alpha-1} E_{\alpha,2\alpha}^2(-\lambda_1^2 t^\alpha)) &= \\ k_1 [\lambda_1^2 t^{2\alpha} E_{\alpha,2\alpha+1}^2(-\lambda_1^2 t^\alpha) + E_\alpha(-\lambda_1^2 t^\alpha) + t^\alpha E_{\alpha,1+\alpha}^2(-\lambda_1^2 t^\alpha) - E_\alpha((1 - \lambda_1^2)t^\alpha)]. \end{aligned}$$

After the above tedious work, we are ready to compare between  $w$  and  $u$ , and their approximations  $\tilde{w}$  and  $\tilde{u}$ , respectively. To evaluate the errors, we introduce the finer grid

$$\mathcal{G}^N = X \cup \{(t_n + t_{n-1})/2 : 1 \leq n \leq N\} \cup \{t_n : 1 \leq n \leq N\}. \quad (39)$$

( $N$  is the number of time mesh subintervals). Thus, for large values of  $N$ , the error measure  $\|v\|_{\mathcal{G}^N} := \max_{t \in \mathcal{G}^N} \|v(t)\|$  approximates the norm  $\|v\|_{L^\infty}$  on the time interval  $(0, 1]$ .

The source term  $w$  satisfies the regularity assumption in (28) for  $\sigma = \alpha$ . Thus, the theoretical error results in subsection 3.3 suggest that  $\|w - \tilde{w}\|_{L^\infty(0,T)} = O((\Delta t)^{\min\{2, \alpha\delta\}})$ . The numerical numbers in Tables 1 and 2 confirm these results for different choices of the fractional exponent  $\alpha$  and of the graded mesh exponent  $\delta$ . For some graphical illustrations of the errors and the positive influence of the graded mesh, see Figures 1 and 2.

We focus next on the graphical comparison between the exact solution  $u$  and its approximation  $\tilde{u}$ . As mentioned earlier, when the parameter  $\gamma < 1$ , the non-local initial condition  $I^{1-\gamma}u(x, t)|_{t=0} = g(x) = 4 \cos(4\pi x)$  leads to unbounded solution  $u$  as  $t \rightarrow 0$ , which is the case here, see (38). If we choose  $\alpha = \gamma = 0.5$ , then the two-parameter derivative  $D^{\alpha,\gamma}$  reduces to the Riemann-Liouville derivative  $D^\alpha = D^{0.5}$ . Figure 3 shows surface plots of both the exact and numerical solutions over graded time meshes with mesh exponent  $\delta = 2$ . We cut off the initial part of the plots since the solution blows up near  $t = 0$ . The surface plots for small  $t$  are shown separately in Figure 4. Surface plots for  $\alpha = 0.5$  and  $\gamma = 0.7$  are shown in Figures 5 and 6.

When  $\gamma = 1$ ,  $I^{1-\gamma}u(x, t)|_{t=0} = u(x, t)|_{t=0} = g(x) = 4 \cos(4\pi x)$ . In this case,  $D^{\alpha,\gamma}$  reduces to the Caputo fractional derivative  ${}^C D^\alpha$ , and the solution is uniformly bounded over the time-space domain. Figure 7 shows the surface plots of  $u$  and  $\tilde{u}$  over graded time meshes with  $\delta = 2$ .

## 6. Concluding Remarks

A numerical scheme for approximating the time-dependent source term is developed. The scheme solves the VIE for the source term and approximates the convolutions needed to calculate the series coefficients for the solution. Due to the singularity

of the solution near  $t = 0$ , a graded mesh is used to improve the convergence rate. We proved analytically and demonstrated numerically that the rate of convergence is of order  $\sigma\delta$ , where  $\sigma$  is the order of regularity of  $w$  and  $\delta$  is the graded mesh exponent.

## Acknowledgment

The authors would like to acknowledge the support provided by King Fahd University of Petroleum & Minerals.

## References

- [1] E. E. Adams and L. W. Gelhar. Field study of dispersion in heterogeneous aquifer 2. *Water Resources Research*, 28:293–307, 1992.
- [2] T. S. Aleroev, M. Kirane, and S. A. Malik. Determination of a source term for a time fractional diffusion equation with an integral type over-determining condition. *Electronic Journal of Differential Equations*, No. 270:1–16, 2013.
- [3] S. Z. Amir and S. Sun. Physics-preserving averaging scheme based on Grünwald-Letnikov formula for gas flow in fractured media. *Journal of Petroleum Science and Engineering*, 163:616–639, 2018.
- [4] D. Baleanu, Z. B. Güvenç, and J. T. Machado, editors. *New Trends in Nanotechnology and Fractional Calculus Applications*. Springer, 2010.
- [5] H. Brunner. *Collocation Methods for Volterra Integral and Related Functional Differential Equations*. Cambridge University Press, 2004.
- [6] H. Brunner, A. Pedaş, and G. Vainikko. The piecewise polynomial collocation method for nonlinear weakly singular Volterra equations. *Mathematics of Computation*, 68:1079–1096, 1999.
- [7] J. R. Cannon, S. Pérez Esteva, and J. van der Hoek. A Galerkin procedure for the diffusion equation subject to the specification of mass. *SIAM Journal on Numerical Analysis*, 24(3):499–515, 1987.
- [8] Y. Cao, T. Herdman, and Y. Xu. A hybrid collocation method for volterra integral equations with weakly singular kernels. *SIAM Journal of Numerical Analysis*, 41:364–381, 2003.
- [9] R. Caponetto, G. Dongola, L. Fortuna, and I. Petráš. *Fractional Order Systems: Modeling and Control Applications*, volume 72 of *World Scientific Series on Nonlinear Science*. World Scientific, 2010.
- [10] X. Chen and Y. M. Chen. Efficient algorithm for solving inverse source problems of a nonlinear diffusion equation in microwave heating. *Journal of Computational Physics*, 132:374–383, 1997.
- [11] N. Cusimano and L. Gerardo-Giorda. A space-fractional Monodomain model for cardiac electrophysiology combining anisotropy and heterogeneity on realistic geometries. *Journal of Computational Physics*, 362:409–424, 2018.

- [12] A. Demir, F. Kanca, and E. Ozbilge. Numerical solution and distinguishability in time fractional parabolic equation. *Boundary Value Problems*, 2015(1):1, Aug. 2015.
- [13] J. Dixon and S. McKee. Weakly singular discrete Gronwall inequalities. *ZAMM Z. Angew. Math. Mech.*, 66(11):535–544, 1986.
- [14] K. M. Furati, O. S. Iyiola, and M. Kirane. An inverse problem for a generalized fractional diffusion. *Applied Mathematics and Computation*, 249:24–31, 2014.
- [15] K. M. Furati, O. S. Iyiola, and K. Mustapha. An inverse source problem for a two-parameter anomalous diffusion with local time datum. *Computers and Mathematics with Applications*, 73:1008–1015, 2017.
- [16] A. B. Gumel. On the numerical solution of the diffusion equation subject to the specification of mass. *Australian Mathematical Society. Journal. Series B. Applied Mathematics*, 40(4):475–483, 1999.
- [17] R. Hilfer, editor. *Applications of Fractional Calculus in Physics*, Singapore, 2000. World Scientific.
- [18] R. Hilfer. Fractional diffusion based on Riemann-Liouville fractional derivatives. *Journal of Physical Chemistry B*, 104(16):3914–3917, 2000.
- [19] R. Hilfer. Fractional time evolution. In *Applications of Fractional Calculus in Physics* [17], pages 87–130.
- [20] X. Hu, L. Zhao, and A. W. Shaikh. The boundary penalty method for the diffusion equation subject to the specification of mass. *Applied Mathematics and Computation*, 186(1):735–748, 2007.
- [21] M. I. Ismailov and M. Çiçek. Inverse source problem for a time-fractional diffusion equation with nonlocal boundary conditions. *Applied Mathematical Modelling*, 40:4891–4899, 2016.
- [22] B. Jin and W. Rundell. A tutorial on inverse problems for anomalous diffusion processes. *Inverse Problems*, 31(3):035003, 2015.
- [23] A. A. Kilbas, H. M. Srivastava, and J. J. Trujillo. *Theory and Applications of Fractional Differential Equations*, volume 204 of *Mathematics Studies*. Elsevier, Amsterdam, 2006.
- [24] R. Klages, G. Radons, and I. Sokolov, editors. *Anomalous Transport: Foundations and Applications*. Wiley, 2008.
- [25] A. Kleefeld, S. Vorderwülbecke, and B. Burgeth. Anomalous diffusion, dilation, and erosion in image processing. *International Journal of Computer Mathematics*, 95(6–7):1375–1393, 2018.
- [26] P. Linz. *Analytical and numerical methods for Volterra equations*. SIAM Studies in Applied Mathematics, SIAM, Philadelphia., 1985.



- [27] F. Mainardi. *Fractional Calculus and Waves in Linear Viscoelasticity*. Imperial College Press, 2010.
- [28] R. Metzler and J. Klafter. The random walk’s guide to anomalous diffusion: a fractional dynamics approach. *Physics Reports*, 339(1):1–77, 2000.
- [29] T. M. Michelitsch, B. A. Collet, A. P. Riascos, A. F. Nowakowski, and F. C. G. A. Nicolleau. Fractional random walk lattice dynamics. *Journal of Physics A: Mathematical and Theoretical*, 50(5):055003, 2017.
- [30] C. A. Monje, Y. Chen, B. M. Vinagre, D. Xue, and V. Feliu. *Fractional-order Systems and Controls*. Advances in Industrial Control. Springer, 2010.
- [31] K. Mustapha. A superconvergent discontinuous Galerkin method for Volterra integro-differential equations, smooth and non-smooth kernels. *Mathematics of Computation*, 82, 2013.
- [32] K. Mustapha and J. K. Ryan. Post-processing discontinuous Galerkin solutions to Volterra integro-differential equations: Analysis and simulations. *Journal of Computational and Applied Mathematics*, 253:89 – 103, 2013.
- [33] M. D. Ortigueira. *Fractional Calculus for Scientists and Engineers*, volume 84 of *Lecture Notes in Electrical Engineering*. Springer, 2011.
- [34] G. Özkum, A. Demir, S. Erman, E. Korkmaz, and B. Özgür. On the inverse problem of the fractional heat-like partial differential equations: determination of the source function. *Advances in Mathematical Physics*, Article ID 476154:8 pages, 2013.
- [35] I. Petráš. *Fractional-Order Nonlinear Systems: Modeling, Analysis and Simulation*. Springer, 2011.
- [36] I. Podlubny. *Fractional Differential Equations*, volume 198 of *Mathematics in Science and Engineering*. Academic Press, 1999.
- [37] T. R. Prabhakar. A singular integral equation with a generalized mittag-leffler function in the kernel. *Yokohama Mathematical Journal*, 19:7–15, 1971.
- [38] K. Sakamoto and M. Yamamoto. Inverse source problem with a final overdetermination for a fractional diffusion equation. *Mathematical Control and Related Fields*, 1(4):509–518, 2011.
- [39] N. Wang, H. Zhou, H. Chen, M. Xia, S. Wang, J. Fang, and P. Sun. A constant fractional-order viscoelastic wave equation and its numerical simulation scheme. *Geophysics*, 83(1):T39–T48, 2018.
- [40] T. Wei and Z. Q. Zhang. Reconstruction of a time-dependent source term in a time-fractional diffusion equation. *Engineering Analysis with Boundary Elements*, 37(1):23–31, 2013.



- [41] F. Yang, C.-L. Fu, and X.-X. Li. The inverse source problem for time-fractional diffusion equation: stability analysis and regularization. *Inverse Problems in Science and Engineering*, 23(6):969–996, 2015.
- [42] L. Zhou and H. M. Selim. Application of the fractional advection-dispersion equation in porous media. *Soil Science Society of America Journal*, 67(4):1079–1084, 2003.

$N$	$\delta = 1$		$\delta = 2$		$\delta = 3$		$\delta = 4$		$\delta = 5$	
10	2.37e-02		2.06e-02		1.52e-02		8.72e-03		4.10e-03	
20	2.30e-02	0.04	1.76e-02	0.23	9.30e-03	0.70	3.46e-03	1.34	1.11e-03	1.89
40	2.21e-02	0.06	1.38e-02	0.35	4.80e-03	0.96	1.21e-03	1.52	2.81e-04	1.98
80	2.10e-02	0.07	9.89e-03	0.48	2.24e-03	1.10	4.04e-04	1.58	7.05e-05	1.99
160	1.97e-02	0.09	6.53e-03	0.60	1.00e-03	1.16	1.34e-04	1.59	1.76e-05	1.99
320	1.81e-02	0.12	4.06e-03	0.68	4.42e-04	1.18	4.43e-05	1.59	4.72e-06	1.94

Table 1: Errors and convergence rates for  $\alpha = 0.4$  and different values of  $\delta$ .

$N$	$\delta = 1$		$\delta = 2$		$\delta = 3$		$\delta = 4$	
10	2.1240e-02		9.4174e-03		2.0410e-03		6.5174e-04	
20	1.8368e-02	0.210	3.8912e-03	1.275	4.7314e-04	2.109	2.3750e-04	1.456
40	1.4620e-02	0.329	1.4617e-03	1.413	1.1443e-04	2.048	6.9103e-05	1.781
80	1.0625e-02	0.460	5.5222e-04	1.404	3.0410e-05	1.912	1.8453e-05	1.905
160	7.1333e-03	0.575	2.1308e-04	1.374	7.9822e-06	1.930	4.7688e-06	1.952
320	4.5350e-03	0.654	8.3305e-05	1.355	2.0444e-06	1.965	1.2111e-06	1.977

Table 2: Errors and convergence rates for  $\alpha = 0.67$  and different values of  $\delta$ .

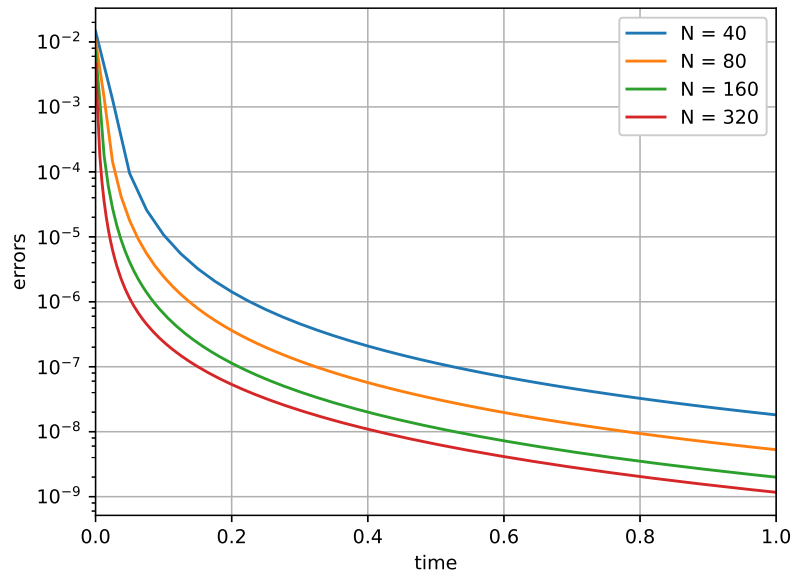


Figure 1: Pointwise errors over a uniform mesh for  $\alpha = 0.67$ .

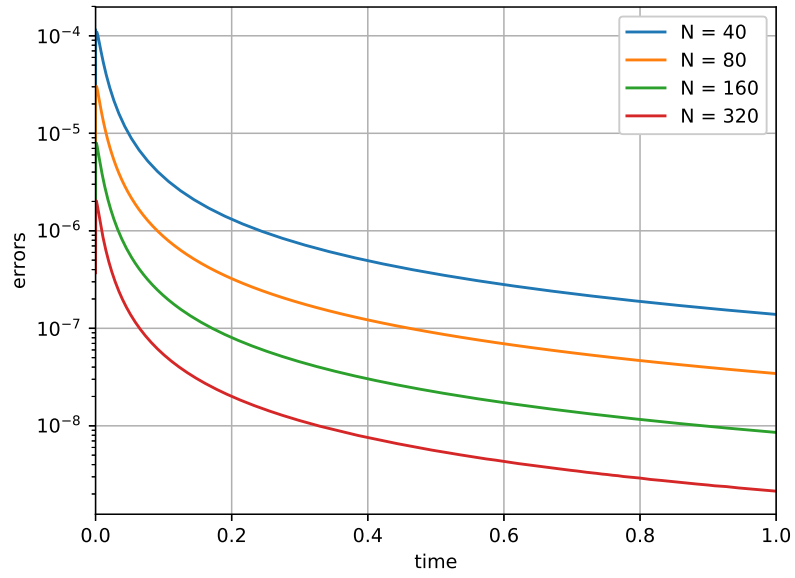


Figure 2: Pointwise errors over a nonuniform mesh of  $\delta = 3$  for  $\alpha = 0.67$ .

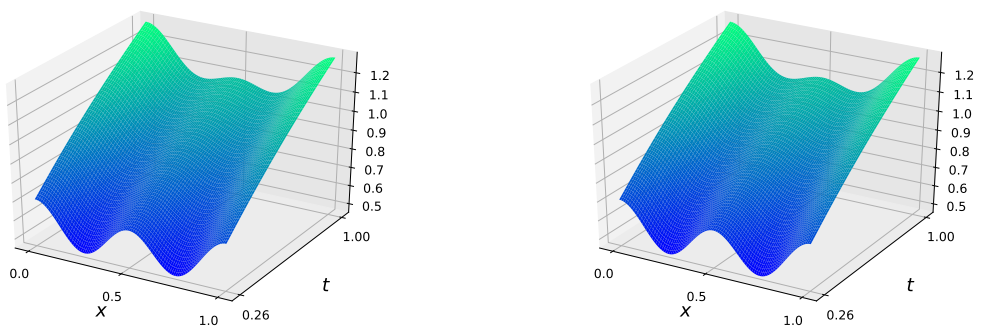


Figure 3: Surface plot of the exact solution (left) and the approximate solution (right) for  $0.26 < t < 1.0$ ,  $\alpha = \gamma = 0.5$  and  $\delta = 2$ .

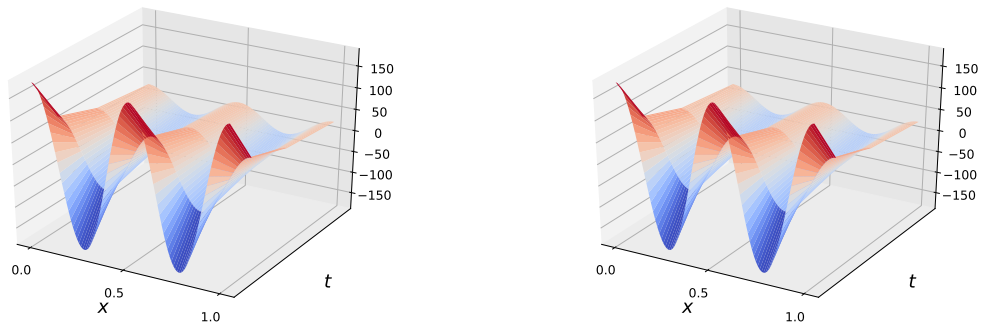


Figure 4: Surface plot of the exact solution (left) and the approximate solution (right) for  $0.1 \times 10^{-3} < t < 1.6 \times 10^{-3}$ ,  $\alpha = \gamma = 0.5$  and  $\delta = 2$ .

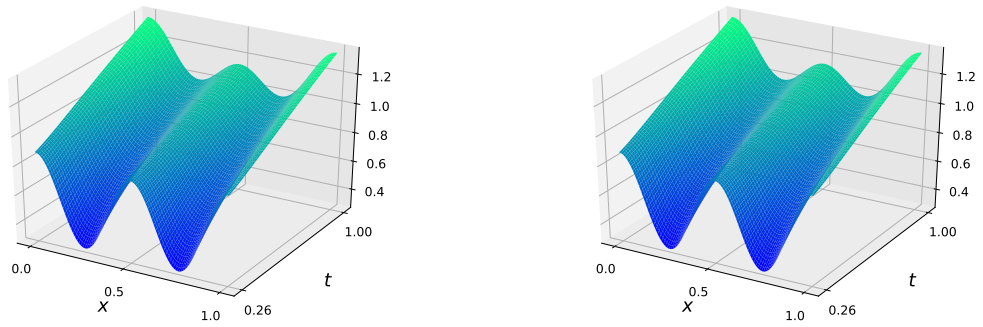


Figure 5: Surface plot of the exact solution (left) and the approximate solution (right) for  $0.26 < t < 1$ ,  $\alpha = 0.5$  and  $\gamma = 0.7$ .

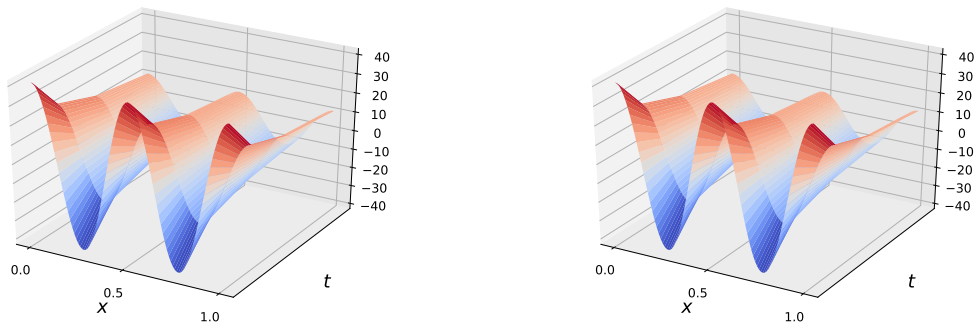


Figure 6: Surface plot of the exact solution (left) and the approximate solution (right) for  $0.1 \times 10^{-3} < t < 1.6 \times 10^{-3}$ ,  $\alpha = 0.5$  and  $\gamma = 0.7$ .

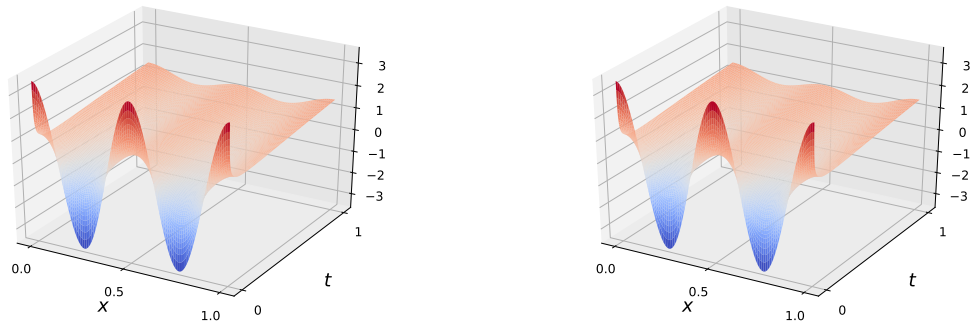


Figure 7: Surface plot of the exact solution (left) and the approximate solution (right) for  $\alpha = 0.5$ ,  $\gamma = 1$  and  $\delta = 2$ .